Rib Support Optimization for a Room-and-Pillar Mine

Khaled Mohamed
Robert Kimutis
Yuting Xue
Gamal Rashed
National Institute for Occupational Safety and Health,
Pittsburgh Mining Research Division

ABSTRACT

The National Institute for Occupational Safety and Health (NIOSH) conducted a monitoring field study to optimize the rib control plan in a room-and-pillar coal mine. The study mine is located in the Central Appalachia coal basin. Two monitoring sites were selected at different sections in the study mine. The selected sites have different overburden depths and geologies. The instrumentation plans at study sites include borehole pressure cells installed at various depths in studied pillars, rib and roof extensometers and load cells mounted on number of the rib bolts. The instrumentation results and observed geology for one of the study sites showed great potential for optimizing the rib bolt plan at that section of the mine. Therefore, a rib support optimization study was followed using numerical modeling technique. A calibrated three-dimensional model was developed using the instrumentation results of the optimization section. The calibrated model was used to determine the optimum rib support for expected overburden depths and rib heights. Baseline rib bolt patterns were assumed for the optimization study. Additional rib bolts, above and beyond the baseline bolting parameters, were outlined and identified as solutions to contain the rib fracturing identified by the modeling results.

INTRODUCTION

In the past several decades, research efforts have focused on roof support. The current rib control practice in U.S. coal mines is to select rib bolts through a trial-and-error approach (Mohamed et al., 2015a). Rib failure incidents can be substantially reduced or even eliminated by adopting an engineering-based coal rib design approach. Coal pillar design is mainly governed by the dimensions of the coal pillar and the applied load. Unlike pillar design, rib stability is a skin control problem in which the local rib composition, such as strength of rib units, cleat density, cleat orientation entry direction with respect to cleat orientation, existence or absence of partings in the coal, and percentage of extracted roof and/or floor rock, and so forth, affects rib stability in coal mines (Mohamed et al., 2015a). Moreover, it is difficult to isolate the effect of a specific factor on the overall rib stability. Therefore, a reliable empirical rib design approach is not achievable because it requires a significant number of case histories to be collected in order to have a reasonable range of all the critical parameters. However, numerical modeling can be a practical tool to assist with rib support design if the modeling is realistic, which can only be achieved through calibration and validation of the numerical model against field data. Numerical model approach is time consuming and requires expertise in numerical modeling, making it unfavorable in practical application. A more practical alternative is to develop a simplified approach using a system of simple linear equations correlating the rib support requirement with its geological and geometrical parameters and overburden depth. This system of linear equations can be achieved by conducting comprehensive parametric studies for the critical parameters using calibrated numerical models. Researchers from the National Institute for Occupational Safety and Health (NIOSH) are developing a coal pillar rib rating (CPRR) technique to measure the integrity of coal ribs Mohamed et al. (2020).

Mohamed, Tulu, and Klemetti (2015b) developed a coal rib model that can rationally calculate rib loading and facture. The coal rib model was calibrated through several field studies (Sears et al., 2017; Zhang et al., 2017; Mohamed et al., 2018; Rashed, Sears, and Mohamed 2019a; Rashed et al., 2019b). As continuation of efforts to calibrate the coal rib model, the current field study was conducted. In the meantime, the field study was used to test the potential of rib support optimization in the study mine. A monitoring field study at two sections was conducted in a room-and-pillar mine that practices retreat mining in the Central Appalachia coal basin. The mined coal seam is the Jawbone seam. The study sections were selected to represent typical geologies and overburden depths in the study mine. Identical instrumentation sites were conducted at each section in the study mine. Rashed, Mohamed, and Kimutis (2020) gave detailed descriptions for the pillar retreat plan and the monitoring results performed at the instrumented sites.

Brief descriptions of the instrumented sites are given in this paper. The instrumentation plan includes load cells (LCs) mounted on

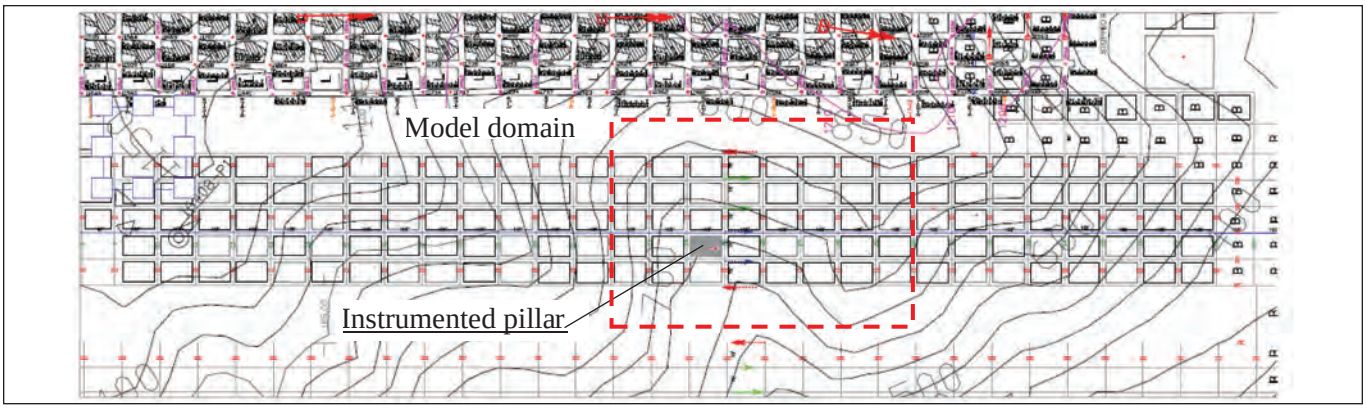

Figure 1. Location of the instrumented pillar in the mine.

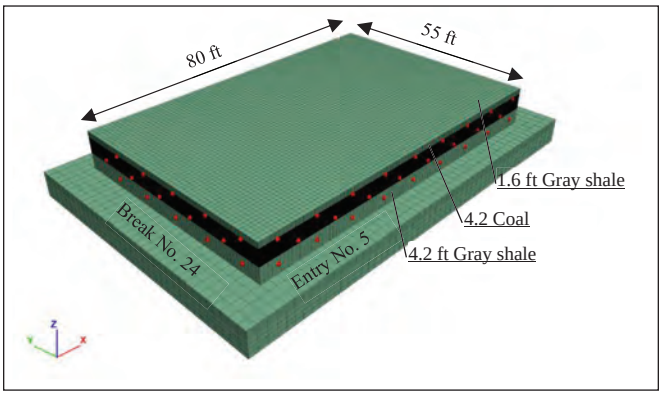

Figure 2. Detailed geometry, lithology, and rib bolts (red solid circles) of instrumented pillar.

rib bolts to monitor the induced loads and borehole pressure cells (BPCs) installed at various depths from the ribs to measure the change in vertical pressure within the pillar during retreat mining. In addition, extensometers were installed in the roof and ribs to monitor the roof and rib movements during the retreat mining process. The monitoring results show that one of the study sections has the potential to be optimized for rib support plan (Rashed, Mohamed, and Kimutis, 2020). A summary of the instrumentation results of the optimization section will be presented in this paper.

The location of the monitoring site in the optimization section is shown in Figure 1. The depth of cover at the monitoring site is about 650 ft. The coal seam is about 4.2-ft thick, which is sandwiched between 1.6-ft-thick slickensided gray shale at the top and 4.2-ft-thick gray shale at the bottom (Figure 2). The slickensided gray shale was mined to avoid weak immediate roof condition. The average rib height at the monitoring site is about 10 ft. The borehole data near the instrumentation site shows that the immediate roof is about 9.3 ft of slickensided sandstone, which cave easily during the retreat mining. The main roof is 63 ft of massive sandstone. Figure 2 shows the dimensions of the instrumented pillar, rib lithology, and the current rib support at the monitoring site. During the development stage, the rib was supported with two rows of 5-ft-long no. 6 fully grouted bolts, grade 60 with 1.5 ft × 1.5 ft–pizza pans, and 8 in. × 8 in.–dome plates.

The monitoring results at the study site are summarized by the following:

1. The maximum vertical stress change in the instrumented pillar caused by the retreat mining was less than 200 psi, and it increased to about 800 psi when the pillar adjacent to the instrumented pillar was being mined.
2. Insignificant rib deformation was recorded on the crosscut side of the instrumented pillar while it was about 0.14 in. on the entry side when the pillar adjacent to the instrumented pillar was mined.
3. The instrumented rib bolts in the entry side of the instrumented pillar showed higher loads than those in the crosscut side. The maximum load on the instrumented rib bolts on the entry side was 3,500 lb (1.6 ton), and it was about 300 lb (0.14 ton) on the crosscut side.
4. The roof extensometers did not show any movements.
5. Good roof caving was observed at the study site when the pillar line was at one and two breaks inby the instrumented pillar.
6. Stress mapping showed insignificant changes in the rib sloughing of the instrumented pillar and the adjacent pillars throughout the study period (Rashed, Mohamed, and Kimutis, 2020). Figure 3 shows photos taken for the entry side of the instrumented pillar in two different dates. Figure 3a is a photo taken right after finishing the installation of the instrument site. Figure 3b is a photo taken when the pillar line was adjacent to the instrumented pillar. The photos show no observable changes in the rib conditions resulting from pillar retreat.

The preceding instrumentation results and field observations demonstrate a great potential for optimizing the rib support plan at that section of the mine. FLAC3D™ (Itasca, 2017) numerical modeling software was used to optimize the rib support design for the study section. A FLAC3D model was built based on the recorded geometry and lithology at the monitoring study. The numerical model was calibrated using the monitoring data by obtaining a comparable field measurements and simulation results. Using the calibrated model, optimized rib bolt patterns were proposed at the study section for expected 7-ft- and 10-ft-high ribs at overburden depths of 500 ft, 600 ft, 700 ft, 800 ft, 900 ft, and 1,000 ft.

(a) Development stage

(b) Pillar retreat line is close to the site

Figure 3. Photos showing rib conditions, at the entry side, at development, and pillar retreat stages.

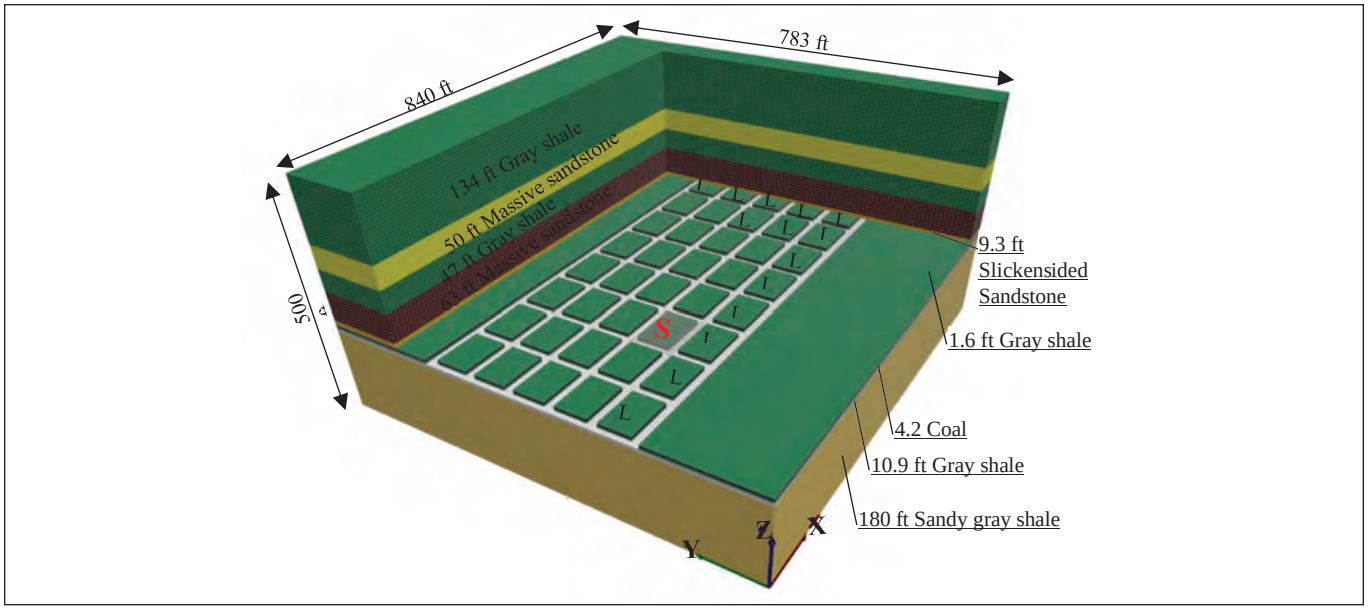

Figure 4. The FLAC3D model for the study site. The instrumented pillar is labeled by the red letter "S," and the unmined pillars are labeled by the letter "L."

BUILDING FLAC3D MODEL FOR THE MONITORING SITE

A FLAC3D model was developed for the monitoring site (Figure 4). The lateral dimensions of the model, represented by the red dashed rectangular lines in Figure 1, were determined in the FLAC3D model to ensure the stress transfer between the instrumented pillar (labeled with "S" in Figure 4) and the surrounding pillars. The model includes five rows of pillars inby the instrumented pillar and two rows of pillars outby the instrumented pillars. Barrier pillars of 200 ft in width are located between the studied panel and adjacent panels. The pillars in the studied panel are 55 × 80 ft rib-to-rib, and the span of the entries and crosscuts is 18 ft. The overall dimensions of the FLAC3D model are 840 × 793 × 500 ft in X, Y, and Z directions, respectively.

The bottom and four sides of the model are constrained by roller supports to constrain the horizontal displacement of the model boundary. A uniform pressure of 361 psi was applied on the top of the model. The maximum horizontal stress was assumed to be parallel to the face cleat direction in the instrumented pillar (Y direction, Figure 4). The maximum and minimum in situ horizontal stress in rock strata were calculated from the equations proposed by G. S. Esterhuizen, Esterhuizen (personal communication, 2017).

$$\sigma_{Hr} = 45.385 + 12.8412 * Z_r + 0.4031 * E_r \quad \text{(Equation 1)}$$

$$\sigma_{hr} = 0.65 * \sigma_{Hr} \quad \text{(Equation 2)}$$

where σ_{Hr} and σ_{hr} are the maximum and horizontal stresses in psi, respectively; E_r is the Young's modulus of rock strata in psi, and Z_r is the depth of rock strata in feet.

The maximum and minimum in situ horizontal stress in the coal seam was estimated with the equations proposed by Liu et al. (2016).

$$\sigma_{Hc} = 170.23 + 11.4144 * Z_c \quad \text{(Equation 3)}$$

$$\sigma_{hc} = 8.5608 * Z_c - 213.875 \quad \text{(Equation 4)}$$

where σ_{Hc} and σ_{hc} are the maximum and horizontal stresses in psi, respectively, and Z_c is the depth of coal seam in feet.

Laboratory tests were conducted on the coal and shale specimens collected from the study site. The average uniaxial compressive strength of coal was 2,278 psi, and the average Young's modulus was 228,582 psi. The coal seam was modeled using the coal-mass model developed by Mohamed et al. (2018). The coal-mass properties used in the FLAC3D model are listed in Table 1. Point load tests were conducted on gray shale specimens collected from the study site. Excluding the minimum and maximum values, the average axial and diametral strengths are 4,106 psi and 13,396 psi, respectively. Zipf (2007) proposed input properties of ubiquitous material properties for different rock types that can be used in FLAC3D models. The results of the point load tests were used to identify the input parameters for rock materials using Zipf's proposed input properties. The mechanical properties of coal and rock that lead to the best match with field measurements are listed in Tables 1 and 2. The properties of the interface between the pillar/roof and pillar/floor are listed in Table 3.

Table 1. Coal-mass properties used in FLAC3D model.

Young's modulus (psi)	228,582
Poisson's ratio	0.25
Intact compressive strength (psi)	2,278
Coal-mass scale	20.0
Fracture plastic shear strain	0.01
Fracture plastic tensile strain	0.001
Joint friction angle (degrees)	25.0
Face cleat dip angle (degrees)	90.0
Face cleat orientation with respect to the mining direction of entry (degrees)	90.0

At the study site, pull-out tests on short-encapsulated rib bolts were conducted to provide the bolt properties in FLAC3D models. Rib bolts were simulated as fully grouted pile elements. Rigid connects between rock bolts and rib were assumed at the bolt segments where the bolts interact the rib. Table 4 summarizes the properties of rib bolts in the FLAC3D model.

CALIBRATION OF FLAC3D MODEL FOR THE MONITORING SITE

FLAC3D model of the monitoring site was solved in three steps:

Step 1. The in situ stress was initialized in the model using Equations 1 through 4 in this geostatic step.

Table 3. Interface properties.

Peak friction (degrees)	30
Peak cohesion (psi)	83
Peak tensile strength (psi)	16
Residual friction (degrees)	14
Residual cohesion (psi)	51
Residual tensile strength (psi)	10
Normal stiffness (psi/in.)	2.88×10^5
Shear stiffness (psi/in.)	9.58×10^3

Table 4. Physical and mechanical properties of the rib bolts used in the model.

Bolt length (in.)	60
Bolt diameter (in.)	0.75
Young's modulus of steel (psi)	29×10^6
Poisson's ratio of steel	0.25
Yield load (lb)	50,582
Grout cohesion (lb/in.)	1,140
Grout shear stiffness (lb/in./in.)	2,400
Grout normal stiffness (lb/in./in.)	2,400
Friction angle (grout) (degrees)	25.0

Table 2. Mechanical properties of rock strata (Zipf, 2007).

Material Name	Description	Lab UCS (psi)	Field UCS (psi)	Young's Modulus (psi)	Cohesion (psi)	Friction Angle (deg)	Dilation Angle (deg)	Tensile Strength (psi)
Initial values of the input parameters for rock materials								
Rock 7	Slickensided sandstone, gray shale	9,135	5,075	1.45×10^6	1,450	30	10	508
Rock 8	Massive sandstone	11,165	6,235	1.74×10^6	1,740	32	10	609
Initial values of the input parameters for bedding planes								
Rock 7	Slickensided sandstone, gray shale	5,945	3,335	1.45×10^6	1,015	27	10	334
Rock 8	Massive sandstone	8,555	4,785	1.74×10^6	1,450	28	10	479

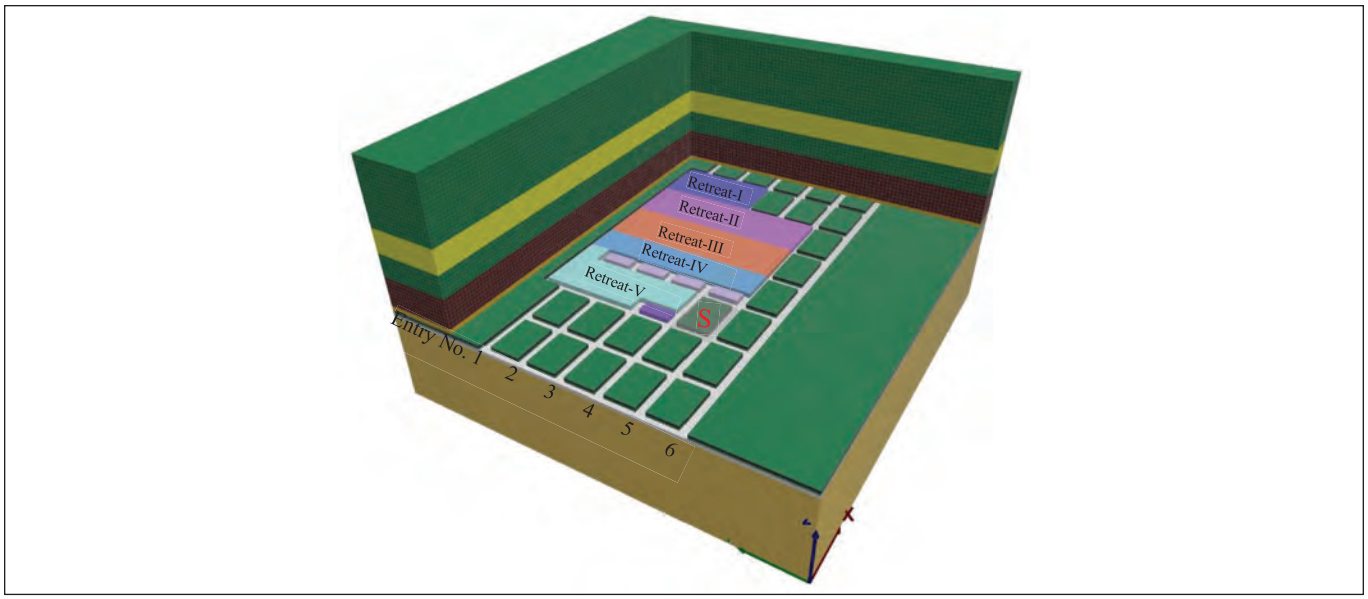

Figure 5. The FLAC3D model showing the sequence of panel retreat and unmined stumps near the instrumented pillar.

Step 2. Entries and crosscuts were developed in this development step.

Step 3. The pillars were extracted in the sequence shown in Figure 5 in this abutment loading step. The pillars between entries 5 and 6 were unmined, and stumps were unmined during pillar recovery. In addition, the caving zone was replaced by gob material after pillar recovery. The gob material was expressed by the model proposed by Salamon (1990) with an initial Young's modulus of 4,466 psi and a maximum gob strain of 0.189. The rock stratigraphy in Figure 4 shows that there is a massive sandstone stratum of 63 ft located 11 ft above the coal seam. It is reasonable to assume that the caving zone cannot extend into the massive sandstone stratum. The reasonable caving height is 19.3 ft between the massive sandstone stratum and the floor.

It is critical to confirm that the material properties and loading conditions of the developed model are rationally representing the rock strata and loading transfer at the study panel. Two sets of FLAC3D models were developed assuming different gray shale properties as defined by Rock 3 and Rock 7 (Zipf, 2007). The first set of models assumed the critical plastic shear strain of 0.01 for coal mass, and the second set assumed the critical plastic shear strain was 0.02. The modeling results were compared with the field measurements at the study site. A calibrated FLAC3D model can be achieved if the model is able to reflect the loading and deformation behavior of the instrumented pillars. As the weakest unit affecting rib stability is the coal seam, close attention was dedicated to match the loading and deformation of the coal seam during the calibration process. In this paper, only the coal and rock properties for the models that showed best match with field measurements, are presented.

The vertical stress, rib displacement, and rib bolt load in the instrumented pillar and roof sag were recorded in the model at the same locations of the study site. These results were recorded at the end of each solution step (geostatic step, development, and abutment loading steps from I to V). The model results after development were used as a reference because the instrumentations were installed when the face was already advanced by three to four breaks inby the study site.

Figure 6 shows the change in vertical stresses in the instrumented pillar at different depth measured from field and compared with model's output. All BPCs were placed in the coal seam. It shows good agreements in vertical stress change between the calibrated model and field measurements in most monitoring locations. For some BPCs, the model slightly overestimated the vertical stress change.

Figure 7 shows the change in the rib displacement at the entry and crosscut sides of the instrumented pillar at the end of each retreating step, I to V. Excluding the gray shale at the entry side, the change in rib displacements calculated by the calibrated FLAC3D model are in acceptable agreement with the field measurements, especially in the coal seam.

Despite the conducted pull-out tests for rib bolts and the rib bolt properties calculated from these tests, the simulated rib bolts in the calibrated model did not successfully resemble the measured bolt load. The FLAC3D model overestimated the induced rib bolt loads, especially in those bolts installed in the coal seam. This discrepancy could be attributed to the crude simulation of the interaction between the bolt head and rib. In the model, rigid connection between the bolt head and coal ribs was assumed. Field observations do not support this assumption. Rational simulation for bolt head/rib interaction maybe required, but it is beyond the scope of this study.

The calibrated FLAC3D model showed no change in roof sag at the entry and crosscut of the study site at the end of retreating step V, which well-matched the field measurements.

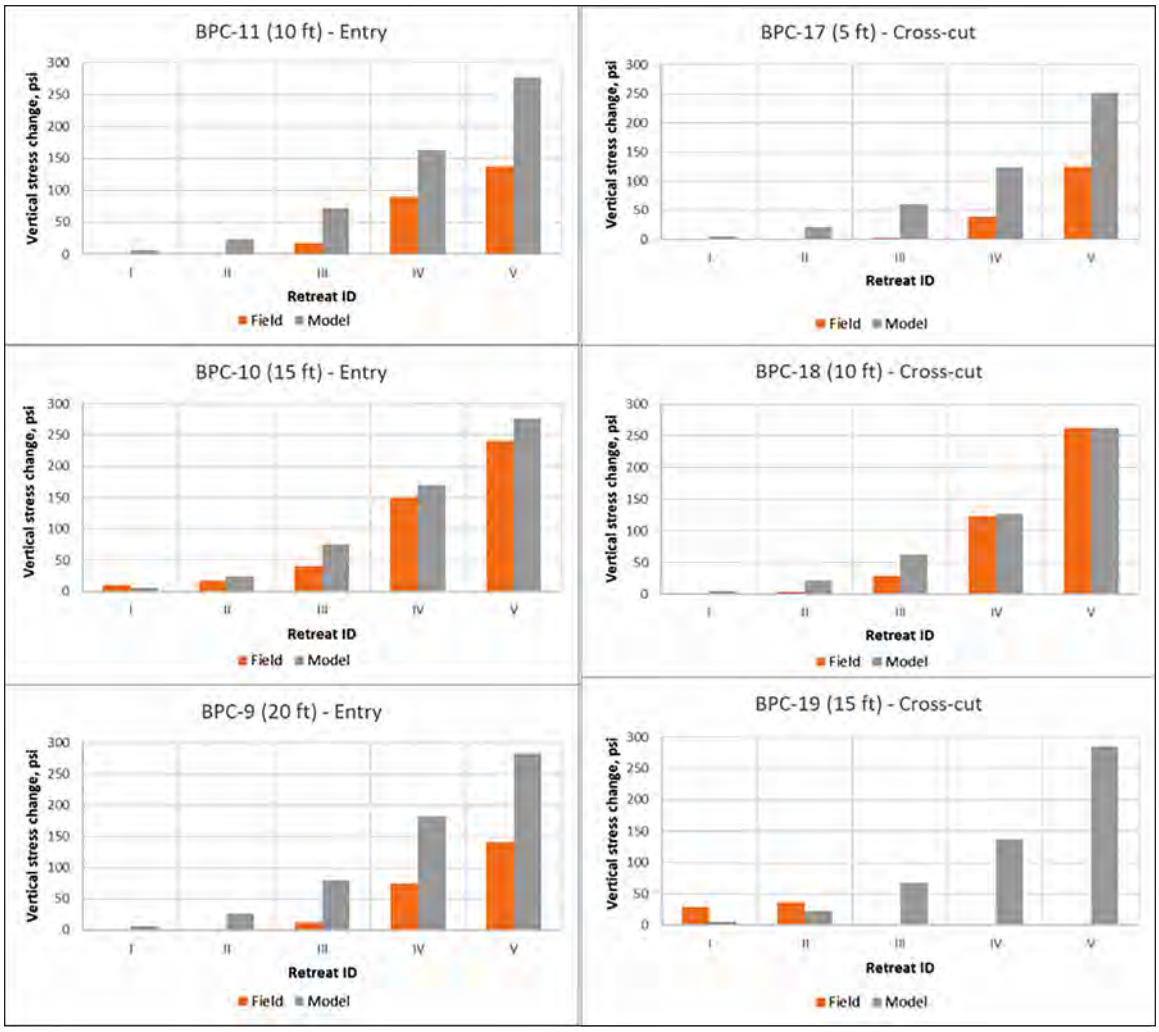

Figure 6. Comparison of the change in vertical stress between field measurements and modeling.

PROPOSED RIB BOLTING PATTERNS FOR THE STUDY SECTION

The calibrated FLAC3D model was used to optimize the rib bolting design in the studied section by assuming that the panel geometry, roof caving, and strength of rib units (coal and gray shale) are consistent in studied section. The calibrated model considered six expected overburden depths (500 ft, 600 ft, 700 ft, 800 ft, 900 ft, and 1,000 ft), and two expected rib heights (7 ft and 10 ft) were assumed for each overburden depth. As shown in Figure 8, the 7-ft rib height is composed of 3 ft of gray shale underlined by 4 ft of coal, and the 10-ft rib height is the same as the instrumented pillar at the monitoring site (Figure 4).

The study mine had a rib support plan in place (see original planes, Figure 8) that has been successful with respect to the health and safety of the miners and had experienced no rib skin failures. Type V bolting pattern is currently applied for 7 ft-high ribs, and type H bolting pattern is applied for 10-ft rib height (Figure 8). The internal goal of the study mine was a rib optimization plan created through instrumentation, data acquisition, and critical data analysis if the data and analytical warranted such a result. Alternative rib support plans (see baseline plans, Figure 8) with less rib support were assumed.

The baseline straight bolting pattern (Figure 8) was assumed for a 7-ft-high rib unless significant rib fracture was encountered. In this case, the original type V bolting pattern was adopted. For 7-ft-high ribs, the bolts are installed at 2 ft from the roof line. Type baseline V bolting pattern (Figure 8) was assumed for the 10-ft-high rib unless significant rib fracture is encountered. In this case, the original type H bolting pattern will be adopted. For the 10-ft-high ribs, the top bolts are installed at one-third of the rib height from the roofline; while the bottom bolts are installed at one-half of the rib height. All rib bolts are fully grouted: 5-ft-long, no. 6, and grade 60. Compared with the original bolting pattern, we can find that the assumed bolting patterns reduced one row of rib bolts. However, additional rib bolts may be required above the baselines based on the simulation results. The coal mass model (Mohamed et al., 2018) can predict the fractures in the coal ribs. As the coal seam is the weakest member in the rib, the extent and location of rib fracture in the coal seam at the pillar between entries 5 and 6 (Figure 5) were used as indicators for the requirement of additional rib support.

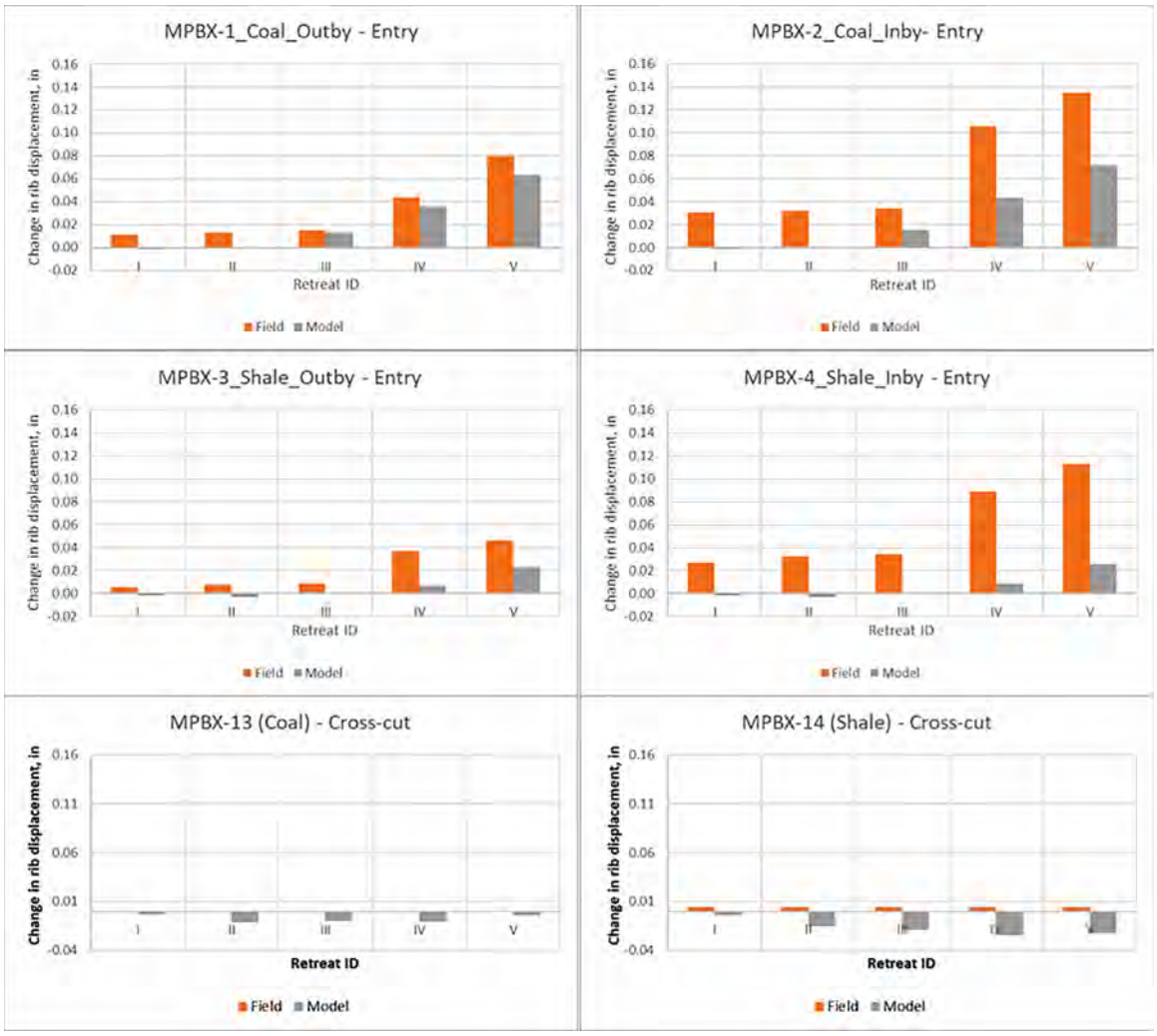

Figure 7. Comparison of the rib displacements between modeling and field measurements with multipoint borehole rib extensometers (MPBXs).

RIB BOLTING PATTERN FOR 7-FT MINING HEIGHT RIBS

Figure 9 shows the predicted rib fractures in the coal seam at the end of retreating step V for each overburden depth with the rib height of 7 ft. Additional rib bolts, above and beyond the baseline (Figure 8), were outlined and identified as solutions to control the rib fracturing identified by the model results as follows:

1. When the overburden depth is 500 ft, there is no fracture in the coal rib, and baseline pattern maybe applicable.
2. For an overburden depth of 600 ft or deeper, there are coal fractures at the pillar corners, and installing additional rib bolts in the coal seam at each pillar's corner is required.
3. When overburden depth increases to 700 ft, the fractures start to propagate along the crosscut sides of the studied pillar, and it is required to install additional bolts in the coal seam at both ends (15 ft from the corners) of the crosscut sides of the pillars.
4. Rib fractures extend through the crosscut side of the rib when the overburden depth reaches 800 ft. Installing additional bolts in the mid-height of the coal seam for the entire crosscut side of the pillars is required.
5. For an overburden depth of 900 ft, rib fractures start to propagate along the entry side in addition to the fracturing of the entire crosscut side rib. It is required to install additional bolts in the mid-height of the coal seam of the pillars for the entire crosscut side and the inby end of the entry side at 18 ft from the corners.
6. When overburden depth increases to 1,000 ft, install additional bolts in the mid-height of the coal seam for the entire crosscut and entry sides of the pillars. This is the original rib bolting pattern. It indicates that when the overburden depth increases to 1,000 ft, the rib bolting density cannot be reduced.

Rib Bolting Pattern for 10-ft Mining Height Ribs

Figure 10 shows the rib fractures in the coal seam at the end of the retreating step V for each overburden depth with the rib height of 10 ft. Additional rib bolts, above and beyond the baseline (Figure 8) were outlined and identified as solutions to control the rib fracturing identified by the model results as follows:

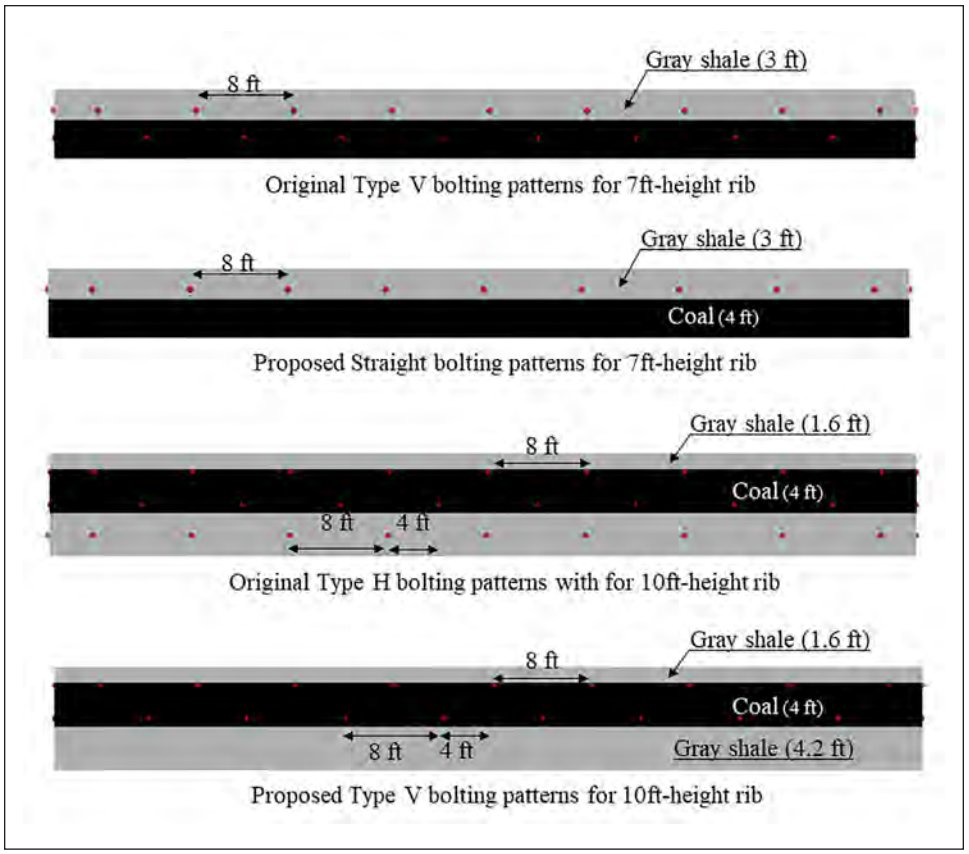

Figure 8. Original and proposed rib bolting patterns.

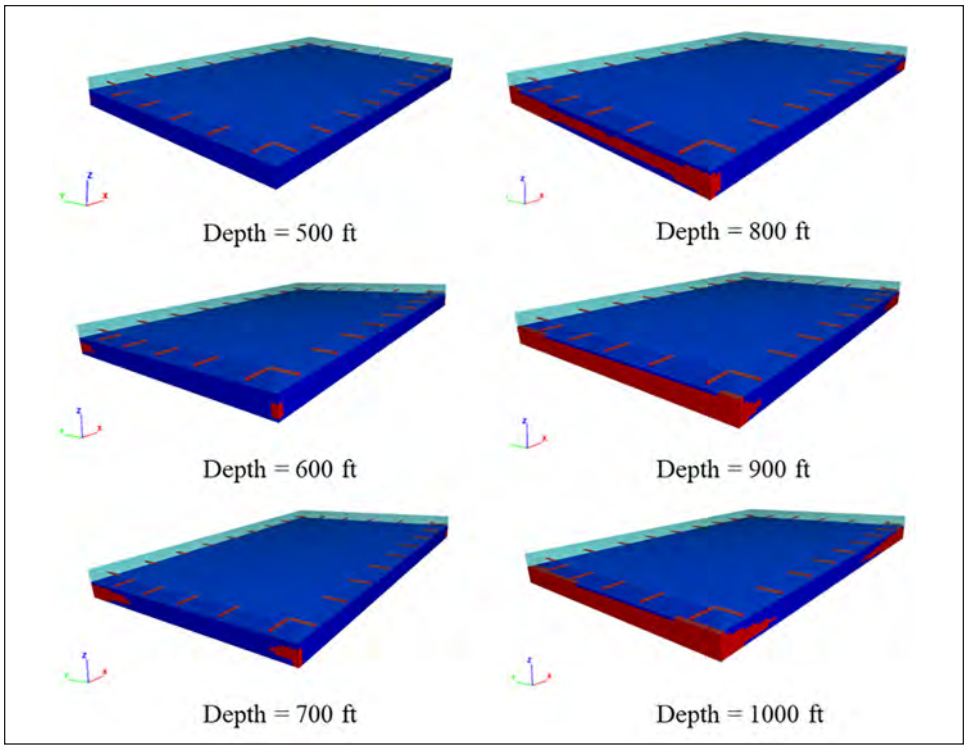

Figure 9. The extent and location of rib fracture (red zone) in the coal seam with 7-ft-high ribs. The rib bolts are marked as red dotted lines.

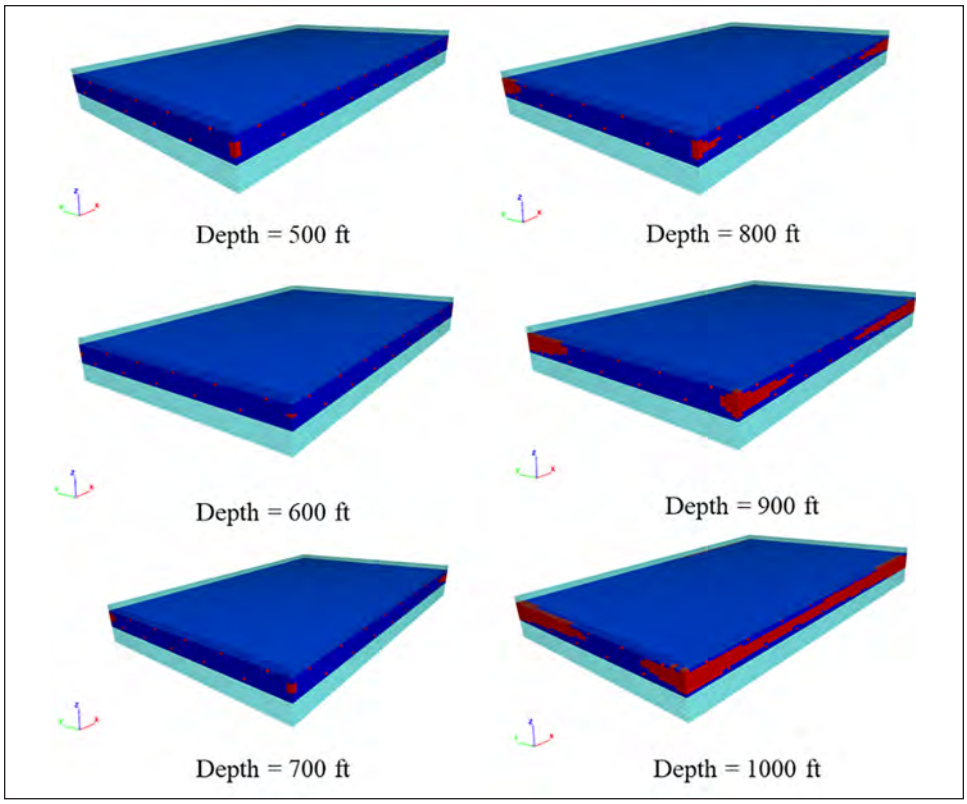

Figure 10. The extent and location of rib fracture (red zone) in the coal seam with 10-ft-high ribs. The rib bolts are marked as red dotted lines.

1. For an overburden depth of 500 ft or deeper, rib fracture only occurs at pillar's corners, and therefore, it is required to install additional rib bolts in the coal seam at each corner of the pillars.
2. When overburden depth increases to 800 ft, install additional bolts at two-thirds of the rib height from the roof line at
   a. Both ends (8 ft from the corners) of the crosscut side of the pillars and
   b. The inby end of the entry side (25 ft from the corners) of the pillars.
3. Coal rib fractures further propagate along both entry and crosscut sides of the pillar when the overburden depth reaches 900 ft. It is required to install additional rib bolts at two-thirds of the rib height from the roof line at
   a. Both ends (8 ft from the corners) of the crosscut side of the pillars,
   b. The inby end of the entry side (46 ft from the corners) of the pillars, and
   c. The outby end of the entry side (15 ft from the corners) of the pillars.
4. Because of the extending rib fractures through both crosscut and entry sides at the overburden depth of 1,000 ft, installation of additional rib bolts at two-thirds of the rib height from the roof line for the entire crosscut and entry sides of the pillars is indicated. The baseline pattern reverts to the original rib bolting pattern, and no reduction for the support density can be done when the overburden depth reaches 1,000 ft.

CONCLUSIONS

NIOSH conducted a monitoring field study at a room-and-pillar mine to understand the load transfer on coal pillars and rib deformation caused by retreat mining and to further determine the potential for rib support optimization.

Two monitoring sites of different geologies were selected in the study mine. The results of one study site showed a great potential for rib support optimization. A FLAC3D model was developed for the rib optimization site and was calibrated with the instrumentation results.

The proposed rib bolt patterns for two rib heights (7 ft and 10 ft) were considered as the baseline. Rib fracturing conditions were investigated with the calibrated model for overburden depths of 500 ft, 600 ft, 700 ft, 800 ft, 900 ft, and 1,000 ft by assuming consistent panel geometry, roof caving, and strength of rib units. Additional rib bolts, above and beyond the baseline bolting parameters, were outlined and identified as solutions to control the rib fracturing identified by the model results.

The simulation results indicate that the rib support can be optimized with overburden depth less than 1,000 ft. However, because of the difference in geologic conditions, the results from this study are only applicable to the studied mine.

ACKNOWLEDGMENT

The authors gratefully acknowledge James Addis and Cynthia Hollerich for helping install the instruments.

DISCLAIMER

The findings and conclusions in this study are those of the authors and do not necessarily represent the official position of the National Institute for Occupational Safety and Health (NIOSH), Centers for Disease Control and Prevention. Mention of any company or product does not constitute endorsement by NIOSH.

REFERENCES

Itasca. (2017). *FLAC3D™*, version 6.0. Minneapolis, MN: Itasca Consulting Group, Inc.

Liu, H., Sang, S., Xue, J., Wang, G., Xu, H., Ren, B., Liu, C., and Liu, S. (2016). "Characteristics of an in-situ stress field and its control on coal fractures and coal permeability in the Gucheng block, southern Qinshui Basin, China." *Journal of Natural Gas Science & Engineering* 36(Part B):1130–1139.

Mohamed, K., Murphy, M., Lawson, H., and Klemetti, T. (2015a). "Analysis of the current rib support practices and techniques in U.S. coal mines." In: *Proceedings of the 34th International Conference on Ground Control in Mining*. Englewood, CO: SME, pp. 83–96.

Mohamed, K.M., Tulu, I.B., and Klemetti, T. (2015b). "Numerical simulation of deformation and failure process of coal-mass." In: *Proceedings of the 49th US Rock Mechanics/Geomechanics Symposium*. Alexandria, VA: American Rock Mechanics Association.

Mohamed, K., Van Dyke, M., Rashed, G., Sears, M., and Kimutis, R. (2020). "Preliminary rib support requirements for solid coal ribs using a coal pillar rib rating (CPRR)." In: *Proceedings of the 2020 International Conference on Ground Control in Mining*. Englewood, CO: SME.

Mohamed, K., Rashed, G., Sears, M., Rusnak, J., and Van Dyke, M. (2018). Calibration of coal-mass model using in-situ coal pillar strength study. ARMA Preprint No. 18-075. Alexandria, VA: American Rock Mechanics Association.

Rashed, G., Sears, M., and Mohamed, K., (2019a). "A case-study of roof support alternatives for deep cover room-and-pillar retreat mining using in-situ monitoring and numerical modeling." In: *Proceedings: SME Annual Conference*. Englewood, CO: SME.

Rashed, G., Mohamed, K., Gearhart, D.F., and Esterhuizen, G.S. (2019b). "Calibration of coal-mass model in a longwall mine: A case study." In: *Proceedings 53rd US Rock Mechanics/ Geomechanics Symposium*. Alexandria, VA: American Rock Mechanics Association.

Rashed, G., Mohamed, K., and Kimutis, R. (2020). "A coal rib monitoring study in a room-and-pillar retreat mine." In: *Proceedings of the 2020 International Conference on Ground Control in Mining*. Englewood, CO: SME.

Sears, M. M, Rusnak, J., Van Dyke, M., Rashed G., Mohamed, K., and Sloan, M. (2017). "Coal rib response during bench mining: A case study." In: *Proceedings of the 36th International Conference on Ground Control in Mining*. Englewood, CO: SME, pp. 67–75.

Salamon, M.D.G. (1990). "Mechanics of caving in longwall coal mining." In: *Proceedings of the 31st U.S. Symposium on rock mechanics*. Golden, CO: Colorado School of Mines, pp. 161–168.

Zhang, P., Mohamed, K.M., Tulu, I.B., and Trackemas, J. (2017). "Coal rib failure and support in longwall gate entries." In: *Proceedings of the 51th US Rock Mechanics/Geomechanics Symposium*. Alexandria, VA: American Rock Mechanics Association.

Zipf, R.K. (2007). "Numerical modeling procedures for practical coal mine design." In: *Proceedings of the International Workshop on Rock Mass Classification in Underground Mine Design*. NIOSH IC 9498. Pittsburgh, PA: National Institute for Occupational Safety and Health, pp. 153–162.

39th International Conference on Ground Control in Mining (ICGCM 2020)

Canonsburg, Pennsylvania, USA
28 - 30 July 2020

Editors:

Ted Klemetti
Brijes Mishra
Heather Lawson
Michael Murphy
Kyle Perry

ISBN: 978-1-7138-1329-3

Printed from e-media with permission by:

Curran Associates, Inc.
57 Morehouse Lane
Red Hook, NY 12571

Some format issues inherent in the e-media version may also appear in this print version.

Society for Mining, Metallurgy and Exploration Inc.
12999 East Adam Aircraft Circle
Englewood, CO 80112-4167

Phone: (303) 948-4200
Fax: (303) 973-3845

cs@smenet.org

Additional copies of this publication are available from:

Curran Associates, Inc.
57 Morehouse Lane
Red Hook, NY 12571 USA
Phone: 845-758-0400
Fax: 845-758-2633
Email: curran@proceedings.com
Web: www.proceedings.com